Theor Chem Acc (2014) 133:1432
DOI 10.1007/s00214-013-1432-y

REGULAR ARTICLE

Effect of CVD diamond growth by doping with nitrogen

Z. Yiming · F. Larsson · K. Larsson

Received: 8 August 2013 / Accepted: 29 November 2013 / Published online: 15 December 2013

Abstract The purpose with the present investigation has been to support and explain the experimental observation made regarding the enhancing effect by N doping on especially the diamond (100)-2 × 1 growth rate. Within the present study, also the commonly observed diamond (111) and (110) surfaces were included, all assumed to be H-terminated. Density functional theory calculations were used, based on a plane wave approach under periodic boundary conditions. It was shown that the surface H abstraction reaction is most probably the rate-limiting step during diamond growth. In addition, the results showed that it is N, substitutionally positioned within the upper diamond surface, that will cause the growth rate improvement, and not nitrogen chemisorbed onto the growing surface in the form of either NH (or NH_2). The here presented numerical value for the growth rate enhancement for the diamond (100)-2 × 1 surface is almost identical with the experimentally obtained one (3.7 vs. 3.6). In addition, the (111) and (110) surfaces were shown to undergo a different growth rate enhancement, with about half as much for the (111) and (110) surfaces as compared to the diamond (100)-2 × 1 surface (1.9, 1.7 vs. 3.7). Despite the rate improvement for all surface planes, this difference will bring about a preferred diamond (100) surface texture.

Keywords Diamond · Growth rate enhancement · CVD · Ab initio theory · N doping

Published as part of a special collection of articles focusing on chemical vapor deposition and atomic layer deposition.

Z. Yiming · F. Larsson · K. Larsson (✉)
Department of Chemistry-Ångström Laboratory, Uppsala University, Uppsala, Sweden
e-mail: karin.larsson@kemi.uu.se

1 Introduction

The diamond material possesses very attractive properties, such as high transparency, high thermal conductivity at room temperature, radiation hardness, as well as an extreme mechanical hardness. In addition, diamond also exhibits superior electronic properties (including high carrier mobility), large electrochemical potential window, low dielectric constant, controllable surface termination, and a high breakdown voltage. Furthermore, when considering the well-known combination of chemical inertness and high degree of biocompatibility [1], diamond became recently a promising candidate for applications like artificial photosynthetic water-splitting, where interfaces between a photo-electrode surface and a redox protein is of utterly importance [2].

Although diamond has been proven to be a genuine multifunctional material, thereby useful for quite many applications, it is still quite expensive to grow it using vapour phase methods like chemical vapour deposition (CVD). However, it has been experimentally proven that e.g. N doping will enhance the diamond growth rate, and thereby reduce the production costs. The influence of nitrogen on the deposition rate has already been reported for both poly- and mono-crystalline diamond [3–6]. Recently, the effect by N on the CVD diamond growth rate enhancement has been studied using laser reflection interferometry [7]. In addition, gaseous N concentrations as low as a few ppm were found to strongly boost up the crystal growth rate in the (100) orientation. As an explanation to this observation, Bar-Yam and Moustakas [8] proposed a defect-induced stabilization of diamond. However, this model does not explain the crystal orientation dependence of the increase in growth rates. More recently, Frauenheim et al. [9] suggested an alternative model, in which donor

electrons originating from sub-surface N will lead to a lengthening of the (100) surface reconstruction bond.

Nitrogen (with its extra electron compared to C) is a well-known n-type dopant, with a very deep donor level in diamond (1.7 eV below the conduction band) [10]. In choosing a suitable donor for diamond, one has, however, not only to consider its donor level but also its solubility and mode of incorporation (e.g. incorporation during growth by in-diffusion or by ion implantation). Impurities have been shown to become introduced into diamond during CVD or HPHT growth [11]. A review article has, in addition, been reporting doping by implantation [12]. A substitutional n-type doping of diamond *during growth* has been of a special interest to study in the present investigation. The resulting substitutional doping will, hence, depend not only on the solubility of the impurity, but will also depend on the kinetics of the growth. Kinetic trapping may then be possible although the final n-type doped product is thermodynamically somewhat unfavourable.

The chemical vapour deposition (CVD) of diamond is a very complex and dynamic process [13]. The growing surface has to be terminated with e.g. H atoms, since it will otherwise collapse to the graphitic phase. However, these terminating species must be abstracted away from the surface to leave room for a growth species (e.g. CH_3). However, in the initial part of the diamond growth process, the abstraction of two surface H species (terminating the surface and one of the H ligands on CH_3) has to take place before any surface migrating can take place, ending with a final incorporation at a step edge. Hence, the process of H abstraction is a very important reaction step during the overall diamond growth mechanism [14]. Since it is an endothermic reaction, whilst the adsorption of e.g. CH_3 highly exothermic (+17 vs. −348 kJ/mol), it is here assumed that the H abstraction is one of the rate-limiting steps for the diamond growth process [15]. Theoretical calculations, using high-level DFT methods, have during the last decade proved to be highly valuable in studying these growth processes on an atomic level. These calculations have proven to be valuable in not only supporting experimental observations, but have also proven to be invaluable in finding the underlying causes to the experimental observations made.

The main goal with the present study has been to support and explain the experimental observations regarding the enhancing effect by N doping on diamond thin film growth rates. The position in the lattice, and the chemical form of the N species, have been of an outmost importance in studying the effect of nitrogen on the growth rate. The three most commonly observed diamond surface planes have been involved in the present study were all were H-terminated; (100)-2 × 1, (111) and (110). The density functional theory (DFT) was used for all of the calculations, based on a plane wave approach under periodic boundary conditions. All results were carefully analysed in order to gain a deeper knowledge about the underlying reasons to the observed growth rate enhancements.

2 Methods

The majority of the calculations in the present study were performed using the CASTEP program from Accelrys, Inc. An ultrasoft pseudopotential density functional theory (DFT) method was thereby used and performed under periodic boundary conditions [16]. More specifically, the spin-polarized general gradient approximation (GGSA [17]) was used, which is based on the PBE functional (Perdew–Burke–Ernzerhof [18]) for electron exchange correlations. It has earlier been shown that the spin-polarized GGA method will give more accurate energy values, as compared to the spin-polarized local density approximation (LDA) method [19–21]. The GGA method usually gives a better overall description of the electronic subsystem, compared to the more simple LDA corrections. The reason is that LDA, which is based on the known exchange–correlation energy of a uniform electron gas, is inclined to overbind atoms and to overestimate the cohesive energy in the system under study. On the contrary, GGA takes into account the gradient of the electron density, which gives a much better energy evaluation. The cut-off energy for the plane waves was set to 240 eV, and the number of k points was (3 × 2 × 1). The Monkhorst–Pack scheme [22] was used for the k-point sampling of the Brillouin zone, which generated a uniform mesh of k points in reciprocal space. The choice of these plane wave parameters was evaluated in test calculations, where a cut-off energy of 240 eV and a k-point set of (1 × 1 × 1) resulted in a change in total energy of 1 % [as compared to the results obtained for a cut-off energy of 200 eV and a k-point set of (3 × 2 × 1)]. However, a more accurate setting with a cut-off energy of 280 eV, and a k-point set of (3 × 3 × 1), resulted in an energy difference of as small as 0.1 %. As a conclusion, a cut-off energy of 240 eV, and a k-point set of (3 × 2 × 1), was found adequate to use in the present study.

Three different super cells, modelling the diamond surface planes (100)-2 × 1, (110) and (111), respectively, have been constructed in the present investigation. The corresponding models are shown in Fig. 1, together with the different ways, N is incorporated in the surface region. All of these surfaces are terminated by H atoms to simulate an as-grown CVD diamond surface. And for modelling the (100) surface, the 2 × 1 reconstructed mono-hydride surface, (100)-2 × 1:H, was used. To improve the

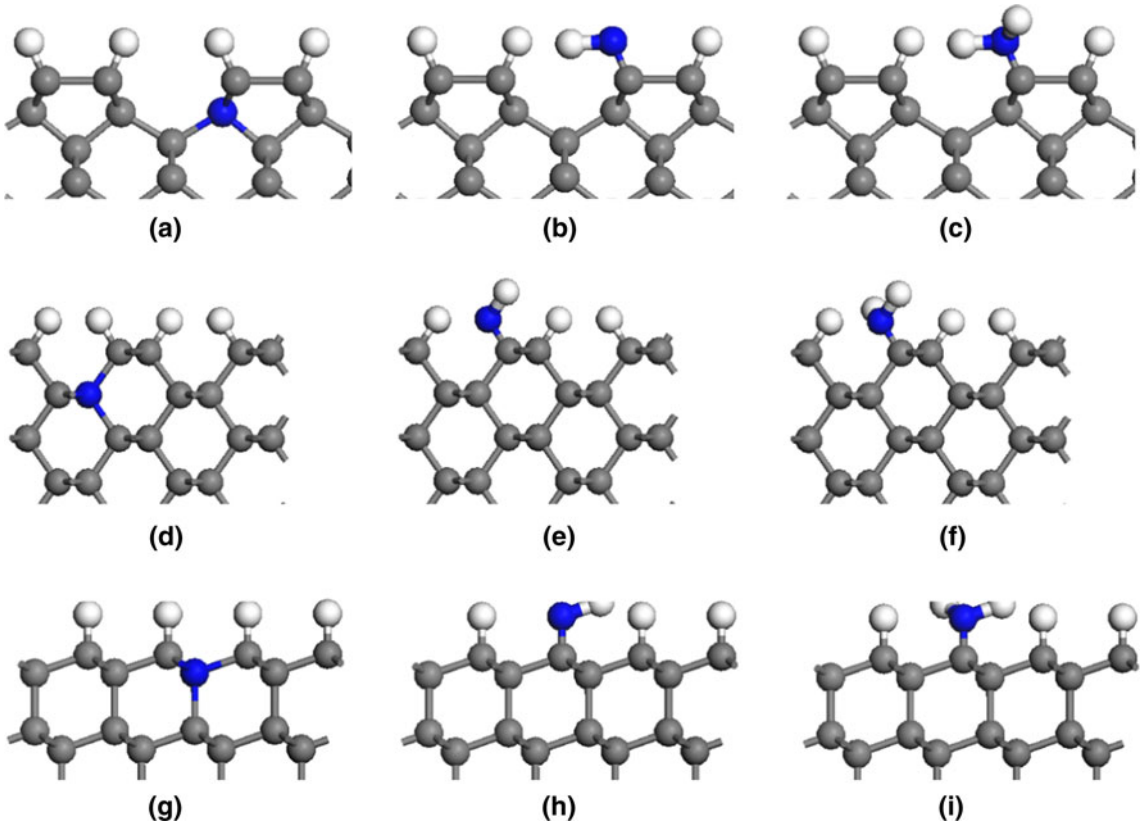

Fig. 1 Representations of nitrogen doping in different diamond surface structures; **a–c** (100)-2 × 1, **d–f** (110), and **g–i** (111). Figures **a**, **d** and **g** demonstrate substitutional doping into the 2nd C atomic layer. Furthermore, **b**, **e** and **h** demonstrate an adsorbed NH radical. Similarly, **c**, **f**, and **i** demonstrate adsorbed NH_2 species

possibilities for more reliable comparisons between the models, all of the unit cells were constructed with the same number of carbon atoms (which is 96). Also, the number of carbon layers was for all unit cells set to six since test-calculations have shown that this thickness is optimal to use in the simulation of the H abstraction process. A further increase in number of layers did not render any visible change in the numerical value for the hydrogen abstraction energy (<0.1 %). The bottom of the diamond slabs was terminated by H to saturate the dangling bonds and to mimic a bulk continuation. All atoms, with an exception for the bottom hydrogen and carbon layer, were allowed to freely relax during the optimization procedure. This geometry optimization procedure was based on the BFGS algorithm [23]. Earlier test-calculations have shown that a 10 Å supercell z-axis is optimal to use in the calculations of this type of system, with the purpose to avoid non-realistic inter-slab interactions [24].

The process of H abstraction was modelled by initially positioning an H radical 4 Å above one of the most reactive surface H adsorbates. This H radical was thereafter approached towards the surface in smaller steps (from 4.0 to 1.0 Å, in steps of 0.2 Å), thereby mimicking the initial growth step of surface H abstraction by gaseous H. For each step, the introduced H radical was fixed during the geometrical optimization of the whole system (in addition to the lowest C layer with its terminated H). When the H radical approached the surface-binding H (at an approximate distance of 1.0 Å), a reaction between these two H atoms started to take place. The processes of desorption of this hydrogen molecule (from the surface) was thereafter studied by monitoring a step-wise removal of the H–H molecule from the surface. As was the situation with the approaching H, one of the H atoms (in H_2) was kept fixed during the geometry optimization processes. By using this procedure, the energy barriers for both the approaching H atom (to the most reactive surface H), and the outgoing H_2 molecule, could be calculated.

3 Results and discussions

3.1 General

As presented in Sect. 1, it has been experimentally proven that e.g. N doping will enhance the diamond growth rate,

and thereby reduce the production costs [25]. However, it is experimentally very difficult to determine in which form N will be efficient in this process. To be more specific, it is experimentally not possible to discriminate between the effect of nitrogen in the form of an N-containing species adsorbed on the surface, or as N substitutionally positioned within the upper part of the diamond surface. For this purpose, high-level DFT calculations have been proven to be most useful. In addition to the growth enhancement effect of the N doping, it has also been shown possible to steer towards the growth of diamond (100) [26].

An issue that has to be highlighted is the catalytic effect by the N dopant. The problem is that a very low concentration of N dopants shall be able to give a more pronounced effect on the overall diamond growth rate. However, it has earlier been shown that the surface hydrogens are very mobile on the diamond surface [27]. Hence, the desorption of an H species nearby the N dopant will immediately be replaced by a neighbouring H species on the surface, causing radical surface C sites at longer distances from the N dopant. In short, the substitutional N dopant will improve both the H abstraction rate and concentration of radical surface C sites, the latter being distributed evenly over the surface.

The present investigation will put an emphasis on proving that the method and methodology used is appropriate and reliable. It will also show that the H abstraction from the surface is the rate-determining step in the overall diamond growth rate. In addition, one of the main goals is to support the experimental observation regarding the effect of nitrogen on the diamond growth rate and to further explain these observations by very careful analyses methods on the electronic level.

3.2 H abstraction rates for growth of non-doped diamond

The energy barriers for step 1 in the H abstraction process (i.e. the barrier for the approaching H atom to the most radical surface-binding H) has in the present work been calculated for three different H-terminated diamond planes; (100)-2 × 1, (110) and (111). The second step in this overall process (i.e. the energy barriers for H–H molecule desorption from the diamond surface) has also been calculated. The resulting diamond growth rate is completely determined by rate-determining steps in the growth mechanism. Since H abstraction from the surface has been found to be endothermic, whilst the adsorption of the growth species CH_3 is highly exothermic (+17 vs. −348 kJ/mol), it is here assumed that the H abstraction is one of the rate-limiting steps for the diamond growth process.

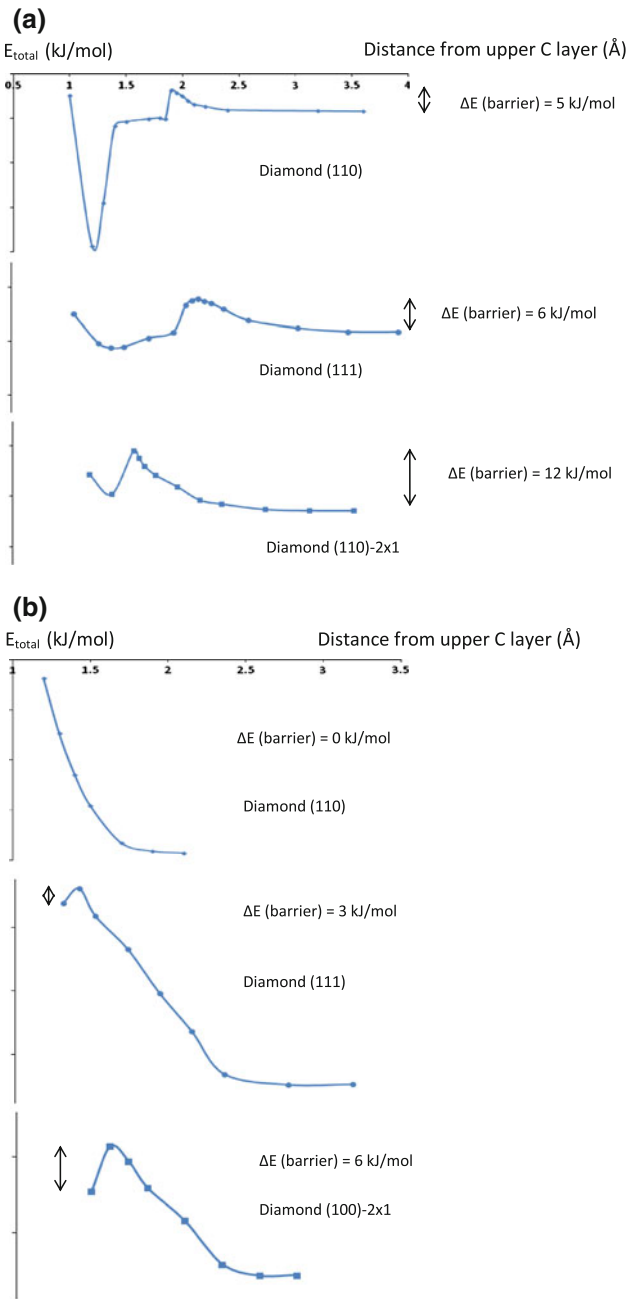

Fig. 2 The energy evolution for an approaching H radical to an H-adsorbate site, as demonstrated for three different surface planes of diamond: (110), (111) and (100)-2 × 1 (**a**). The corresponding desorption of H_2 from the surfaces is shown in (**b**). Both barrier energies, as well as the distances of the transitions states from the surface H adsorbates, are shown in **a** and **b**

Figure 2a shows the energy evolution for an approaching H radical to an adsorbed H species on the surface for the three different surface planes of diamond; (110), (111) and (100)-2 × 1. The corresponding desorption of H_2 from the surfaces is shown in Fig. 2b. The respective barrier energies, as well as the distances of the transitions states

(i.e. energy maxima) from the H adsorbate at the surface, are especially shown in the Figures. As can be seen in Fig. 2a, at a distance of about 3.0 Å from the H adsorbate, an energy barrier is starting to appear and the total energy of the systems starts to increase to a maximum. In order to ensure the accuracy in the position of these maxima, shorter steps (0.05–0.10 Å instead of 0.2 Å) were chosen in the regions surrounding these stationary points. The position of the transition states with respect to the H adsorbates was found to differ appreciably; 1.6, 2.0 and 1.9 for Å for diamond (100)-2 × 1, (111) and (110), respectively. And this observation is not due to the fact that the H adsorbates have undergone relaxation to various extents. In addition, the numerical values of the respective energy barriers were calculated using $\Delta E = E_{\text{maximum}} - E_{\text{furthest away}}$, which also gave quite different values for the various surface planes (12, 6 vs. 5 kJ/mol, respectively).

When continuing the calculation after the energy barriers, and hence with H approaching even closer to the H adsorbate at the diamond surface, the results also looks different depending on the surface plane. As can be seen in Fig. 2a, for the (100)-2 × 1 plane, the energy value directly drops to energy minima. For the situation with the diamond (111) plane, the energy value reduces gradually. This behaviour is even more pronounced for the (110) plane, where the total energy value will first decrease rapidly, followed by a slow decrease that will end by a more dramatic decline to the lowest energy minima. These variations in energy evolution are strongly coupled to structural changes at the surface as a result of the approaching H species.

Despite the variations in energy evolution for the incoming H radical to the surfaces, all of these three planes showed the lowest total energy minimum for a distance of 1.2–1.4 Å from the surface-binding H species. At this distance, the H radical is interacting with this H adsorbate, but to various extents depending on surface plane (as can be seen in Fig. 3). When the approaching H comes close enough to the adsorbed H (for all three diamond planes), an electron population (as the result of a bond population analysis) was observed between the approaching H and the terminating one, being a strong indication of an H–H interaction in the form of bond covalence. For the (110) surface, this bond population will continue to increase as the H–H distance becomes smaller (and a simultaneous decrease in bond population for the C–H bond), with the final formation of gaseous H_2 (se Fig. 3b). The resulting value of bond population for H–H in H_2 is much larger than the electron bond population for the final C–H entity (0.73 vs. −0.04), indicating the C–H bond has been broken completely.

For the diamond (111) surface, the approaching H radical finds an energy minima at a position above the diamond surface where the H–H electron population has increased to a stabilized value of approximately the same size as the one for the C–H bond (0.55 vs. 0.45). On the contrary, the H–H electron population for the (100)-2 × 1 surface will only increase very little when the H species is further approached to the diamond surface [0.24 (H–H) vs. 0.72 (C–H)], finally trapped in a local energy minimum (Fig. 3a). In summary, it is only the approach of a radical H to the diamond (110) surface that will immediately result in the release of H_2. As will be discussed below, an energy barrier has to be overcome for the H_2 molecule to be able to leave the diamond (111) and (100)-2 × 1 surfaces.

The second step in the abstraction process, which involves the removal (i.e. desorption) of H_2 from the surface, has also been calculated for diamond (111), (110) and (100)-2 × 1 (see Fig. 2b). As shown above, no energy barrier was observed for diamond (110) since the approaching H radical will directly induce the removal of H_2 from the surface. In addition, only a minor energy barrier (3 kJ/mol) was observed to be necessary for the removal of an H_2 molecule from the (111) surface. But to desorb a chemisorbed H species in the form of an H_2 molecule from the (100)-2 × 1 plane, a larger energy barrier is needed (6 kJ/mol). This larger energy barrier can be explained by the differences in bond populations for C–H versus H–H at the position of the energy minimum. As presented above, the bond population for the C–H bond is as high as 0.72, which has to break in forming gaseous H_2 molecules. The corresponding value for the (110) surface is 0.45.

When comparing the barrier energies for the approaching H radical, with the one for the desorption of H_2 from the surface, it is obvious that the barrier energies for the desorption of H_2 (step 2 in the desorption process) are smaller than that for the adsorption of the approaching

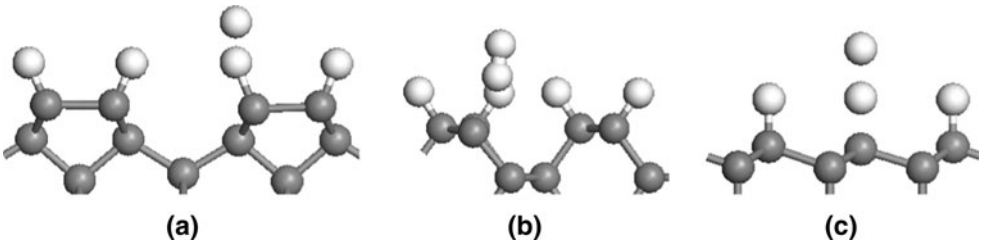

Fig. 3 Structural geometries at the energy minima for an approaching IH radical to a surface-terminating H species, for the different diamond planes: (100)-2 × 1, (110) and (111)

Table 1 Comparison between experimental and theoretical growth rates for the surface planes (110), (111) and (100), respectively

Plane	Growth rate (μm/h)	Relative growth rate (experimental)	Energy barrier (kJ/mol)	Relative growth rate (theoretical)
110	0.24	1.9	4.73	2.4
111	0.19	1.4	6.06	2.0
100	0.13	1.0	11.83	1.0

All values are related to the smallest growth rate [i.e. for (100)]

radical H (step 1). For the various surface planes (111), (100)-2 × 1 and (110), it is less than 50, 62, and 100 %, respectively. The conclusion that can be drawn from this observation is that it is only the adsorption part of the abstraction process which will be the dominating one in determining the H abstraction reaction rate (being identical to the total growth rate since the H abstraction is here assumed to be the rate-determining elemental reaction during diamond growth).

In addition to the barrier energies for the different H abstraction processes, Table 1 also gives information about the relative growth rates (with respect to the slowest one) under the assumption that H abstraction is a rate-limiting growth step. Moreover, it is only the barrier for the approaching H radical that has been used for the rate estimations as presented in the table. The Arrhenius relation has been used for this purpose to make a careful estimation of the growth rate ($v = v_0 \cdot e^{-\Delta E/RT}$), under the assumption that the pre-exponential factor, v_0, is almost identical for the different surface planes. T is the temperature during diamond growth, R is the universal gas constant and ΔE is the barrier of energy for the abstraction process. The relative H abstraction rate, and thereby relative diamond growth rate, can be rewritten as $v_1/v_2 = e^{(\Delta E2 - \Delta E1)/(RT)}$.

In addition to calculated values, also experimentally determined growth rates for the various diamond planes are presented in Table 1. Chu et al. [25] investigated the growth of different diamond planes and also presented different kinetic curves for each plane. For this purpose, they used a hot-filament CVD technique at a substrate temperature of 600–1,000 K, together with a methane mole fraction of 0.4 %. Chu et al. used surface kinetic control during CVD growth of diamond, which means that the diamond growth rate will be determined by the activation energy of the rate-determining step. This circumstance makes it ideal to add theoretical modelling and simulations for support and explanations. As can be seen in Table 1, the experimental diamond growth rates at 700 °C were found to be 0.13, 0.19 and 0.24 μm/h for diamond (100), (111) and (110), respectively. These absolute values correspond to the relative numbers 1.0, 1.4 versus 1.9.

As can be seen in Table 1, the experimentally observed trend in diamond growth rate is identical to the order of H abstraction rates, as carefully estimated from our theoretical calculations; (100) < (111) < (110). There are though some minor differences when comparing the experimental and theoretical relative rates strictly numerically. However, considering the large number of parameters that may influence the growth rate experimentally, these small differences are acceptable. Moreover, the large similarity in relative H abstraction rates with relative experimental growth rates will strongly support the conclusion that H abstraction is indeed a rate-determining step in the growth mechanism of diamond (111), (100) and (110).

When comparing experimental results with calculated ones, the identity in trends and large similarity in numerical values will furthermore justify the theoretical method and methodology used in the present study (both for the present system and the present problem at hand).

3.3 H abstraction rates for growth of N-doped diamond

As was presented in Sect. 1, the introduction of nitrogen into the CVD reaction chamber has been found to induce an increased diamond growth rate. For instance, Dunst et al. [7] were studying the effect of diamond growth by introducing nitrogen into a microwave plasma-activated CVD reactor in depositing single crystalline diamond (100) at 800 °C. The results of that study state that the introduction of N_2 will improve the diamond growth rate with a factor of approximately 2.5 at a CH_4 concentration of 2 %. However, the underlying cause to this growth improvement was not clear; Did N has this effect when incorporated into the diamond lattice or was the effect induced by chemisorbed N-containing species? The main advantage with theoretical DFT calculations is that surface processes, including the breakage and formation of bonds will be most carefully calculated, and the main aim with the present study has been to understand the influence by nitrogen onto the diamond growth rate on an atomic level of theory. The nitrogen dopant has, thereby, either been substitutionally positioned into the upper diamond lattice or has been chemisorbed onto the surface in the form of NH or NH_2 (the formed being a radical).

3.3.1 N substitutionally positioned into various C atomic layers

At first, the effect by substitutionally positioning N within different C atomic layers close to the surface had to be evaluated. For this purpose, both the H adsorption energy and surface H abstraction energy were chosen to be calculated for both diamond (111) and (100)-2 × 1 surface planes. As can be seen in Fig. 4, these two surfaces show

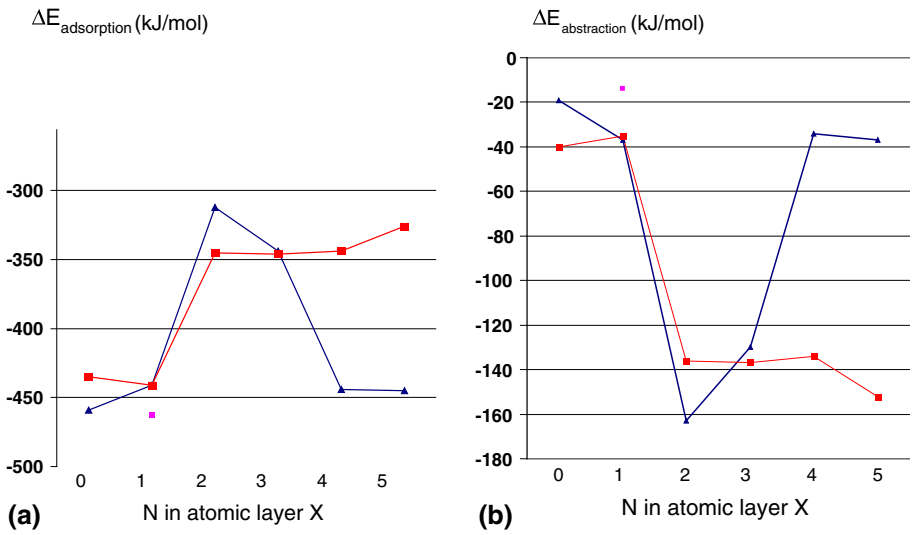

Fig. 4 Variation in H adsorption energy (**a**) and surface H abstraction energy (**b**), when positioning N in different atomic C layers. The energy values at $X = 0$ represent non-doped diamond surfaces. The *squared dots* represent diamond (111) and the *triangular dots* represent diamond (100)-2 × 1

completely different behaviour. However, the trends for H adsorption energy (Fig. 4a) and H abstraction energy (Fig. 4b) show, as expected, similar, but mirrored, results. For the (100)-2 × 1 surface, there are peaks in the adsorption curves for the position of N within C layers 2 and 3 in the upper diamond surface. Hence, the H adsorption process becomes less energetic feasible, whilst the H abstraction becomes much more exothermic. Two different factors have in the present study been found to be responsible for this effect. When positioning N within the second, or third, atomic C layer in an otherwise completely H-terminated diamond (100)-2 × 1 surface, the extra electron in N will occupy the anti-bonding state within one N–C bond. This will result in the breakage of the N–C bond, which, however, will re-bind again after the H abstraction from the surface (with the formation of an electron pair at the vacant surface position). This rather severe surface reconstruction is not possible to take place when positioning N further down in the diamond surface (from the fourth atomic layer, and deeper below). From this explanation, it is clear that N naturally will improve the abstraction process and show a negative effect on the adsorption process. For the H adsorption process, the values are the following: −458 (non-doped) to −319 (N in 2nd layer) kJ/mol. The corresponding values for the surface H abstraction process are −41 (non-doped) to −138 (N in 2nd layer) kJ/mol.

For the diamond (111) surface, it is obvious that the N element will have a strong effect for the C surface layers 2–5. Numerically, these dopant effects are of the same size for all layers. For the H adsorption process, the values are the following: −434 (non-doped) to −349 (N in 2nd layer) kJ/mol. The corresponding values for the surface H abstraction process are 19 (non-doped) to −165 (N in 2nd layer) kJ/mol. For this specific diamond surface, the only dopant effect is the electron transfer towards the C (surface)–H bond, thereby weakening it. As was also the situation with the (100)-2 × 1 surface, an electron pair will be formed on the radical C atom as a result of the H abstraction process. There is a clear indication that this effect also will become less pronounced with an increase in distance from the surface.

Based on all of these calculations, it has been proven reasonable to continue the investigation in the present study by positioning the N dopant within the 2nd atomic surface layers.

3.3.2 *N substitutionally positioned within the C atomic layer 2*

Nitrogen, substitutionally positioned within the second C layer of various diamond surface planes, was here chosen since it was found that this is a position that has a large effect on the H abstraction reaction, and hence on the surface reactivity in general. To analyse this effect on the surface reactivity, Fukui function calculations were performed with the intention to localize the surface sites that are most susceptible towards a radical attack. As can be seen in Fig. 5, there is a major effect by the substitutionally positioned N dopant on the radical susceptibility of the surfaces (100)-2 × 1, (110) and (111), respectively. This effect is more delocalized for the (110) surface, whilst the others show a more local, but still very strong, effect (local means close the N dopant).

Based on the Fukui function calculations, the position of H radical attack onto the H-terminated diamond surfaces was determined from Fig. 5. An identical methodology, as for the non-doped diamond surfaces, was followed in trying to estimate the energy barriers for the H abstraction processes (see Sect. 3.2). The values of H abstraction

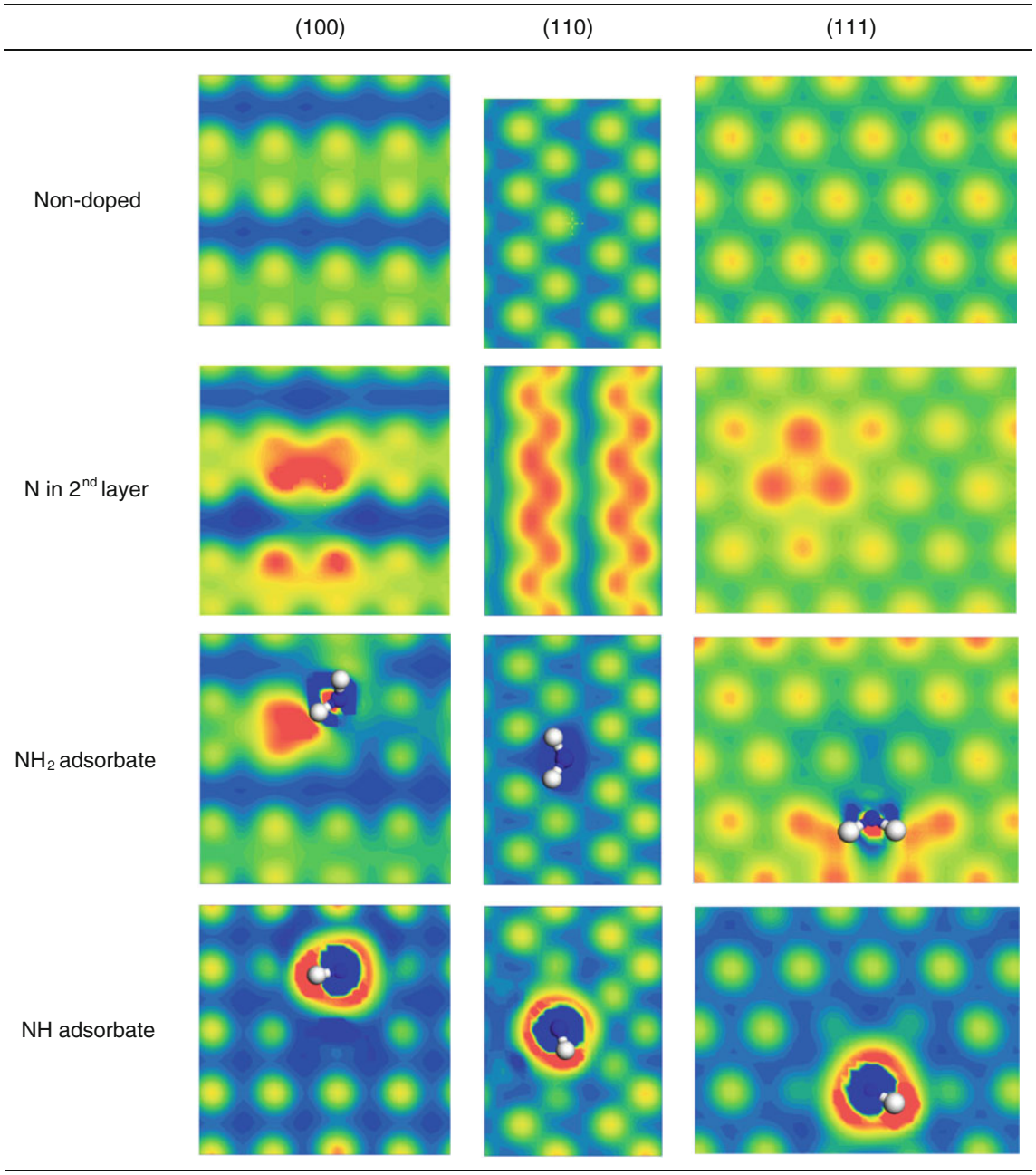

Fig. 5 Isosurface maps of Fukui functions showing the distribution of radical susceptibility for the diamond surfaces [(100), (110), (100)-2 × 1] and for various dopant situations. The *red colour* visualizes the most susceptible part on the surface and the *blue colour* represents the least susceptible part

energy barrier for the different diamond surface planes, and for different kinds of nitrogen doping, are shown in Table 2. The most interesting result is obtained for substitutionally nitrogen doping in the second C atomic layer, for which there is no energy barrier (for the approaching H radical) for any of the surface planes investigated.

The question is now to explain this theoretical observation. Nitrogen has an extra valence electron compared to carbon, and it is at first very important to get information about where this extra electron density will be positioned. Spin electron density calculations have shown that the density from this extra electron will be more globally distributed amongst the bonds in the vicinity to N for the diamond (100)-2 × 1 surface (see Fig. 6a).

Electron deformation densities have also been calculated with the purpose to investigate the effect of N dopants on the individual bonds within the H-terminated diamond surface (i.e. atom–atomic interactions) within the systems.

Table 2 Effect of N on the surface H abstraction energy and relative growth rate (in relation to the respective non-doped surface planes: (110), (111) versus (100)-2 × 1

	Energy barrier (kJ/mol)	Relative growth rate
110		
Non-doped	4.7	1.0
N in 2nd layer	0	1.7
NH_2 adsorbate	5.7	0.9
111		
Non-doped	6.1	1.0
N in 2nd layer	0	1.9
NH_2 adsorbate	6.0	1.1
100		
Non-doped	11.8	1.0
N in 2nd layer	0	3.7
NH_2 adsorbate	8.2	1.5

As can be seen in Fig. 7a, the bond population analysis supports these results, showing that the extra spin will cause a weakening of both the N–C (layer 1) (0.55) and C–H (0.63) bonds. The former one is to be compared with the N–C (layer 3) bonds: 0.60 versus 0.65. And the later with the C–H bonds for non-doped diamond: 0.88. It is thereby obvious that the extra electron in the N dopant (positioned in the 2nd C atomic layer) will weaken the absolute upper part of the diamond (100) surface, and it is assumed that this is also the case for diamond (111) and (110).

The electron deformation densities were also calculated for the approaching H radical at a so called transitions state (TS) distance from the diamond (100)-2 × 1 surface (i.e. identical to the TS distance for non-doped diamond). As can be seen in Fig. 7b, there is a strong interaction between the incoming H and the surface H. There is an electron density between these two atoms (0.18), indicating an electron orbital overlap. In addition, there has been a partial electron transfer to the approaching H radical, and there is a weakening of the C–H bond (from 0.90 to 0.72). All of these values do strongly support the zero-level barrier energy value for abstraction of H from the three different diamond surfaces.

3.3.3 *N chemisorbed onto the surface in the form NH or NH_2*

Since it was not experimentally clear in what form nitrogen will aid for the improved diamond growth rate, nitrogen was attached to the surface in the form of a radical NH group (i.e. chemisorbed onto the diamond surface). As can be seen in Fig. 6b, the non-paired electron will stay locally at the adsorbate NH place. This local position of the extra electron is further supported by the deformation density results in Fig. 7b. The extra electron in NH does not show any tendency to interact with the surface in weakening bonds by filling anti-bonding orbitals. Due to this reason, the barrier energy for the H abstraction is expected to be very similar as for the non-doped diamond surfaces, and these calculations have hence not been included in the present study.

However, when nitrogen is chemisorbed in the form of NH_2 onto the diamond surface, the situation becomes more complex (even though NH_2 is not a radical species when adsorbed to the diamond surface). For the (100)-2 × 1 surface plane, the reactivity of the surface hydrogen in the vicinity to one of the hydrogen atoms within the NH_2 group is enhanced. The situation with the (110) plane is quite different in that the reactivity close to NH_2 becomes weakened. For the situation with the (111) plane, it will be similar to the situation for the (100)-2 × 1 plane. The reactivity of the surface hydrogen closest to the hydrogen atom in the NH_2 group will be reinforced whilst the one closest to the nitrogen atom will decrease in reactivity. However, these changes in surface reactivity are apparently not large enough to affect the H abstraction barrier energy (see Fig. 5; Table 2). The usefulness with these Fukui

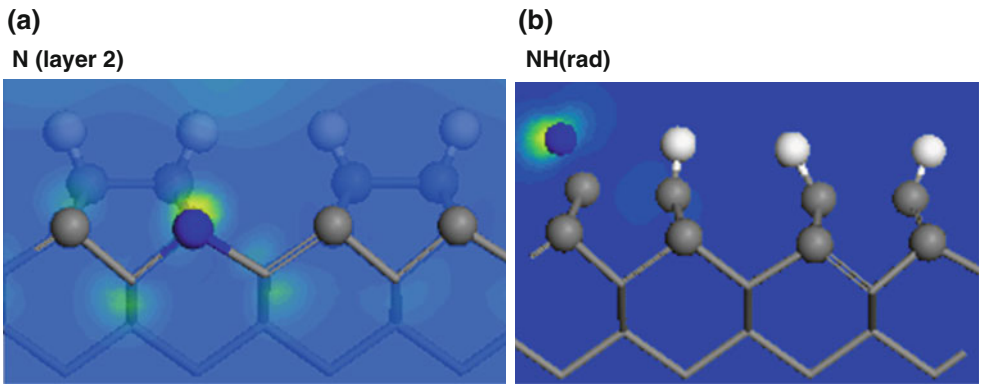

Fig. 6 Demonstration of the electron spin density for diamond (100)-2 × 1, with N substitutional positioned within the 2nd C atomic layer (**a**), or chemisorbed in the form of a radical NH species (**b**)

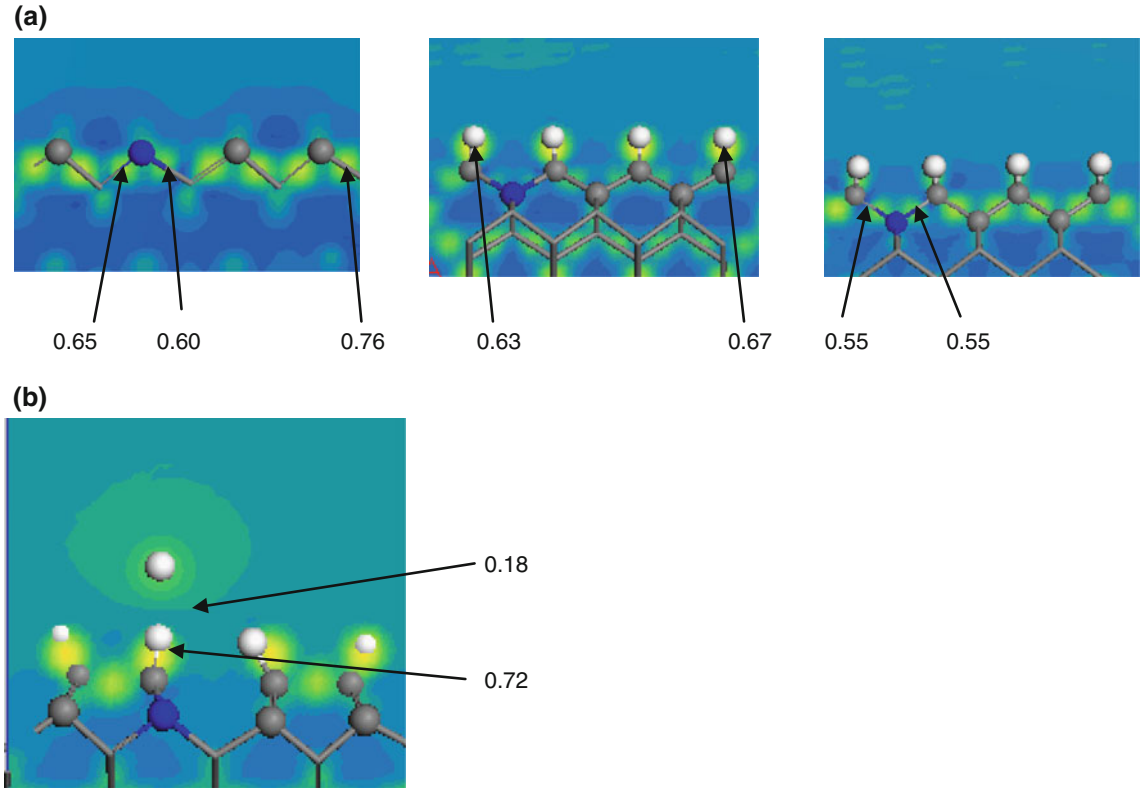

Fig. 7 Electron density difference maps showing the dopant-induced lattice weakening (**a**) and the interaction between the approaching H and the surface H atom (**b**)

maps is that they are visualizing the most reactive surface H atoms, whereto the gaseous H shall be approached.

Similar to the situation with NH adsorbates, the nitrogen doping in the form of NH_2 adsorbed do not show any larger effect as compared to the non-doped scenario. To be more specific, the H abstraction energy barriers for the diamond (100)-2 × 1 and (111) planes were observed to decrease, whilst the barrier for the (110) plane increased; NH_2 doping (8, 6, 6) versus non-doping (12, 6. 5) (see Table 2). However, it must be stressed that these difference are marginal for diamond (111) and (110). There is also a correlation observed between these changes in activation energy and the effect by NH_2 doping on the surface reactivates. The Fukui function maps for the diamond (100)-2 × 1 and (111) planes show a slight improvement in surface reactivity, whilst the corresponding one for the (110) plane show a decrease in reactivity (see Fig. 5). However, as stated above, these effects are relatively small and there is no effort put in trying to understand this correlation in the present work.

3.3.4 Theoretical versus experimental results regarding growth improvement by N doping

As was the situation in Table 1 for non-doped diamond, the energy barrier values for the various N doping situations can be used in forming ratios of diamond growth for the various diamond surface planes (see Table 2). In the Arrhenius relation used for this purpose, the temperature, T, was set to 1,073 K since this is the substrate temperature that was used in the experimental work that the present study is referring to [7]. Moreover, the experimental work did only consider the effect by N doping on the diamond (100)-2 × 1 growth. A comparison with experimental results for the situation with N doping can, hence, only be done for this specific surface. It is also in Table 2 assumed that the H abstraction step is the rate-determining one in the growth of diamond, which in this study has been shown to be a very realistic conclusion.

As is quite clear from Table 2, there is a remarkable increase in growth rate when introducing N within the 2nd C atomic. This is especially the situation for the diamond (100)-2 × 1 surface, where a growth enhancement has been calculated with a factor of 3.7, compared to the non-doped scenario. The experimental growth rate enhancement for diamond (100)-2 × 1 was found to depend on the combination of N_2 and CH_4 concentration in the MWPA-CVD reaction chamber, with a maximum value of 3.5 [7]. Hence, there is an almost perfect resemblance between the here calculated factor and the experimentally observed one. This result is first of all a justification of the theoretical

methods and methodology used in the present study. Secondly, it also strongly supports the general assumption that the H abstraction process from the diamond surface is the rate-limiting step in the complete diamond growth mechanism. At last, the very good correspondence between theory and experiments confirm the experimental observation and takes a step further in making the assumption that it is most probably N, incorporated in the lattice, that is responsible for the observed growth rate enhancement.

As can be seen in Table 2, the theoretically obtained growth rate enhancements for the (111) and (110) surfaces were not that pronounced as that for the (100)-2 × 1 surface (1.9, 1.7 vs. 3.7). However, they were still appreciable. For the situation with NH_2 chemisorbed onto the surface, instead of being positioned with the upper lattice, only a minor effect will be observed for the diamond (100)-2 × 1 surface. However, the calculated growth enhancement by a factor of 1.5 will not explain the experimental value of 3.5. Further analysis is, however, necessary in order to analyse the effect of NH_2 more in detail.

4 Summary and conclusion

It has experimentally been proven that nitrogen doping will enhance the single crystalline diamond (100) CVD growth rate by a factor of 3.5 at a CH_4 and N_2 concentration of 2 atomic percentage versus 100 ppm in a MWPE CVD chamber. However, it is experimentally very difficult to determine in which form N will be efficient in this process; as substitutionally positioned within the lattice, or as adsorbed on the surface in the form of NH or NH_2. Hence, it has been proven quite necessary to complement with theoretical DFT calculations to be able to learn as much about the underlying causes that would be necessary for a deeper understanding on the electronic level. The present investigation has had the focus to use high-level DFT calculation in order to discriminate between the effects of diamond growth by nitrogen within the lattice, or chemisorbed to it, for H-terminated diamond (100)-2 × 1, (111) and (110) surface planes. The main goal has been to both support the experimental observations and to be able to understand why nitrogen has this specific effect on the diamond growth rate.

The effect on the H abstraction energy barrier by positioning N within different C layers was at first calculated in the present study. It was obvious that it is only N within either the 2nd or 3rd C atomic layer, where the N doping show any effect on the surface reactivity. As a result, all following calculations with N within the diamond lattice were performed with N in the 2nd C layer. In addition, a validation by the methods and methodologies used in the present study has been performed by comparing the calculated enhancement of growth rate by the experimental one and also by comparing the variations in diamond growth rate for the planes (100)-2 × 1, (111) and (110). The very good agreement in ratios did clearly show that both the methods and methodologies used are adequate to use for the present type of system.

The calculation of diamond growth rates have been made by assuming that the H abstraction process is the rate-determining step in the overall growth mechanism. It has also been verified in the present work that this also is the situation. As was the situation with verifying the chosen method and methodology, this verification was based on the comparison between earlier experimental observations and the here presented theoretical work, both for the effect of N doping and for the variation surface planes.

The results of the present investigation do clearly support the experimental finding that N_2 within the MWPE CVD chamber will enhance the mono-crystalline diamond (100) growth rate by a factor of 3.7. The corresponding calculated growth rate enhancement for the diamond (111) and (110) surfaces were found to be much lower, but still appreciable: 1.9 versus 1.7. Careful analysis within the present study has clearly shown that it is N substitutionally positioned within the upper diamond surfaces that will cause the growth enhancement effect. In contradiction, N in the form of either NH or NH_2 has been shown to not be responsible for the improved growth rate.

The experimental observation of an improved growth rate for the diamond (100) surface plane is strongly supported by the theoretical results, which showed that the increase in growth rate is about twice as high for the (100) surface, as compared with the (111) and (110) surfaces.

This investigation is the first in a series of studies where the effect of various dopant elements will be studied: N, B, P, S O and Si. The main goal is to learn as much as possible about the effect of either an excess or depletion of electrons within the diamond system and based on this deeper knowledge be able to tailor-make and develop novel dopant systems for even higher deposition rates and/or lower deposition temperatures.

Acknowledgments This work was supported by the Faculty of Uppsala University, and the Swedish Research Council (VR). The computational results were obtained using CASTEP from Accelrys.

References

1. Amaral M et al (2008) J Biomed Mater Res A 87:91
2. McEvoy JP, Brudvig GW (2006) Chem Rev 106:4455

3. Cao GZ et al (1996) J Appl Phys 79:1357
4. Muller-Sebert W et al (1996) Appl Phys Lett 68:759
5. Yan CS, Vohra YK (1999) Diam Relat Mater 8:2022
6. Liu T, Raabe D (2009) Appl Phys Lett 94:21119
7. Dunst S, Sternschulte H, Schreck M (2009) Appl Phys Lett 94:224101
8. Bar-Yam Y, Moustakas TD (1989) Nature 342:786
9. Frauenheim T (1998) Diam Relat Mater 7:348
10. Bachelet GB, Hamann DR, Scluter M (1982) Phys Rev B 26:4199
11. Kalish R (2001) Diam Relat Mater 10:1755
12. Kajihara SA et al (1991) Phys Rev Lett 66:2110
13. Liu H, Dandy D (1996) Diamond chemical vapor deposition. Elsevier, Amsterdam
14. Spear K, Dismukes J (1994) Synthetic diamond: emerging CVD science and technology. Wiley, London
15. Van Regemorter T, Larsson K (2008) Chem Vap Depos 14:224
16. Segall MD et al (2002) J Phys Condens Matter 14:271
17. Perdew JP, Burke K, Ernzerhof M (1996) Phys Rev Lett 77:3865
18. Perdew JP, Burke K, Wang Y (1996) Phys Rev B 54:16533
19. Perdew JP et al (1992) Phys Rev B 46:6671
20. Ziesche P, Kurth S, Perdew JP (1998) Comput Mater Sci 11:122
21. Van Regemorter T, Larsson K (2008) J Phys Chem A 112:5429
22. Monkhorst HJ, Pack JD (1976) Phys Rev B 13:5188
23. Pfrommer BG et al (1997) J Comput Phys 131:233
24. Petrini D, Larsson K (2005) J Phys Chem B 109:22426
25. Chu CJ et al (1992) Novel Forms Carbon 270:341
26. Tallaire A et al (2013) Physique 14:169
27. Larsson K, Carlsson J-O (1999) Phys Rev B 59:8315